

- (27) Chu, D. Y.; Thomas, J. K. *Macromolecules* **1987**, *20*, 2133.
 (28) Strauss, U. P. In *Microdomains in Polymer Solutions*; Dubin, P., Ed.; Plenum: New York, 1985; pp 1-12.
 (29) Gelman, R. A.; Barth, H. G. In *Water-Soluble Polymers*; Glass, J. E., Ed.; ACS Symposium Series 213; American Chemical Society: Washington DC, 1986; p 101.
 (30) Cang, C. P. V. Private communication, University of Toronto.
 (31) Ben-Naim, A. *Hydrophobic Interactions*; Plenum: New York, 1980. Tanford, C. *The Hydrophobic Effect: Formation of Micelles and Biological Membranes*; Wiley: New York, 1980.
 (32) Winnik, F. M. *Macromolecules* **1989**, *22*, 734.
 (33) Nowakowska, N.; White, B.; Guillet, J. E. *Macromolecules* **1988**, *21*, 3430.
 (34) Halary, J. L.; Monnerie, L. In *Photophysical and Photochemical Tools in Polymer Science*; Winnik, M. A., Ed.; D. Reidel: Dordrecht, Holland, 1986; pp 589-610.
 (35) See for example: Chandar, P.; Somasundaran, P.; Turro, N. *J. Macromolecules* **1988**, *21*, 950.

Longest Relaxation Times of Linear Polymers in Concentration Regions between the Critical Concentrations for Zero-Shear Viscosity and for Steady-State Compliance

Yoshiaki Takahashi,* Michio Wakutsu, and Ichiro Noda

Department of Synthetic Chemistry, Nagoya University, Furo-cho, Chikusa-ku, Nagoya 464-01, Japan. Received May 1, 1989; Revised Manuscript Received July 3, 1989

ABSTRACT: The longest relaxation times τ_m of linear polymers in concentration regions between the critical concentrations for the zero-shear viscosity η^0 and for the steady-state compliance J_e , that is, in a semidilute region for η^0 and in a dilute (not entangled) region for J_e , were studied by measuring the stress relaxation after cessation of steady shear flow. It is concluded that the weight-average relaxation time τ_w ($= \eta^0 J_e$) is well represented by τ_m and the magnitudes of the contribution of the terminal relaxation processes to η^0 are the same in semidilute solutions for η^0 , whether the entanglements are effective to J_e or not.

Introduction

The longest relaxation time τ_m , which is a measure of the time required to free a whole molecule from the restraints imposed, is one of the central problems in the study of viscoelastic properties of polymer chains in entangled regions.^{1,2} Hence, τ_m or, more in detail, the terminal relaxation spectra³⁻⁵ as well as other viscoelastic parameters such as the zero-shear viscosity η^0 and the steady-state compliance J_e ⁶⁻⁸ have been extensively studied. In concentrated solutions and melts where polymer chains are highly entangled with each other, the terminal relaxation processes can be well separated from the faster processes owing to the high entanglement densities. In the highly entangled regions, the viscoelastic properties at the terminal relaxation process, so far published, can be summarized as follows^{1,2}

$$\eta^0 \propto M^{3.4} C^b \quad (1a)$$

$$J_e \propto M^0 C^{-2} \quad (1b)$$

$$\tau_m \propto M^{3.4} C^{b-2} \quad (1c)$$

where M and C are the molecular weight and the concentration of the polymer, respectively, and b is the exponent specifying the concentration dependence of zero-shear viscosity. As shown in these equations the weight-average relaxation time τ_w defined as the product of η^0 and J_e can be well represented by τ_m .^{1,3} Moreover, these relaxation times are found to be related to the characteristic time specifying the onset of non-Newtonian viscosity.^{1,6}

The entanglements decrease with decreasing concentration, and the effects of entanglements on viscoelastic properties disappear at certain critical concentrations,

which are different in different properties.^{1,2,8} As shown in the molecular weight-concentration diagrams for η^0 and J_e of linear polymers in good solvents in previous papers,^{7,8} the critical concentrations from dilute to semidilute regions for η^0 and from dilute (not entangled) to entangled regions for J_e , denoted by C_c^η and C_c^J , respectively, are given by

$$(C_c^\eta)^{1.27} M = 1.55 \times 10^4 \quad (2a)$$

$$(C_c^J) M = 1.4 \times 10^5 \quad (2b)$$

These relationships can be also read as the corresponding critical molecular weight-concentration relationships. If we compare the critical concentrations or the critical molecular weights for η^0 with those of J_e , the latter is 4-6 times higher than the former.^{7,8}

In the concentration region between the two critical concentrations, i.e., in semidilute solutions for η^0 and in dilute solutions for J_e , τ_w is proportional to $M^{4.4}$ instead of to $M^{3.4}$, since η^0 is proportional to $M^{3.4}$ while J_e is still proportional to M in this region. Moreover, the concentration dependence of τ_w is also different above and below C_c^J , according to the change in the concentration dependence of J_e (C^{-2} to C^{-1}). We already reported that the characteristic time for the onset of non-Newtonian viscosity is proportional to τ_w also in this weakly entangled region, where the entanglements are effective to η^0 but not to J_e .⁹ However, it has not been studied whether τ_w is represented by τ_m or not in this region. The purpose of this work is, therefore, to study the relationships between τ_w and τ_m in the region.

Experimental Section

Samples used here were linear polystyrenes with narrow molecular weight distributions purchased from Tosoh Corp. Molec-

Table I
Molecular Characteristics of Samples

sample code	$10^4 M_w$	M_w/M_n
F-40	35.5	1.02
F-80	71.0	1.05
F-128	126	1.05
F-380	384	1.04

ular characteristics of the samples are listed in Table I.

A good solvent for polystyrene used here is benzyl *n*-butyl phthalate (BBP) purchased from Tokyo Kasei Co. Ltd. Its purification method and physical properties were reported previously.¹⁰

Weighed amounts of sample and solvent were mixed at about 50 °C and gently stirred several times per day for about 1 month until the solutions became uniform. Polymer concentrations were converted to gram per deciliter assuming the additivity of the specific volumes of sample and solvent.

Primary normal force difference and shear stress under steady shear flow and shear stress relaxation after cessation of steady shear flow were observed with a Weissenberg rheogoniometer Type R-17 of Sangamo Controles Ltd., equipped with a gapservo system. A cone-and-plate geometry with a 4° angle and a 5-cm diameter was used. Measurements were carried out at 50.0 ± 0.1 °C. The stress relaxation after cessation of steady shear flow was continuously recorded on an electromagnetic recorder. The reliability of measurements with the Weissenberg rheogoniometer Type R-17 was confirmed as reported previously.^{11–13}

Results

Steady shear viscosity and compliance were calculated from the shear stress and primary normal stress difference observed under steady shear flow. The zero-shear viscosity η^0 and the steady-state compliance J_e were determined by extrapolating these observed data to the zero-shear rate as described previously.⁶ The η^0 and J_e data obtained here and also the τ_w data calculated from η^0 and J_e are listed in Table II.

Figure 1a shows double-logarithmic plots of $\eta_{sp}^0/M^{3.4}$ against C , where $\eta_{sp}^0 = (\eta^0 - \eta_s)/\eta_s$ and η_s is the solvent viscosity. It is apparent that all data are on a straight line drawn with a slope of 5. Therefore, the molecular weight and concentration dependence of η_{sp}^0 can be expressed as

$$\eta_{sp}^0 \propto M^{3.4} C^5 \quad (3)$$

in the concentration region in this experiment. The concentration dependence of η_{sp}^0 is slightly higher than that in good solvents reported in previous papers ($C^{4.3}$).^{8,9} This discrepancy may be due to the difference in the solvent power, and BBP used here may be a slightly poorer solvent for polystyrene. The difference in the concentration dependences, however, will not affect the following discussion, since the relationship between τ_m and τ_w is concerned here.

Table II
Viscoelastic Properties of Polystyrenes in *n*-Butyl Benzyl Phthalate in Semidilute Region

sample code	$10^2 C$, g·cm ⁻³	η^0 , Pa·s	$10^5 J_e$, Pa	$10^2 \tau_w$, s	$10^2 \tau_m$, s	$\tau_m G_m$, Pa·s	$\tau_m G_m / \eta^0$
F-40	23.80	90.6	1.38	1.25	3.62	57.9	0.64
	26.86	211	1.32	2.79	7.36	171	0.81
F-80	16.31	127	3.95	5.02	10.6	82.6	0.65
	18.04	177	3.82	6.76	15.7	120	0.68
	21.64	280	3.73	10.4	19.0	200	0.71
F-128	9.83	37.6	15.9	5.98	12.2	19.9	0.53
	11.01	74.2	11.2	8.31	16.7	57.9	0.78
	11.85	102	10.8	11.0	19.9	74.4	0.73
F-380	2.93	6.95	149	10.4	16.2	3.48	0.50
	3.75	18.3	149 (109) ^a	27.0 (20.0) ^a	37.0	9.51	0.52

^a The values in parentheses are calculated by using the average value of J_{eR} .

Double logarithmic plots of $J_e C$ against C are also shown in Figure 1b. Since J_e is found to be almost independent of solvent power, the data in this work can be directly compared with that in good solvents reported previously.⁸ The solid line denotes the J_e data in good solvents in entangled regions, while the dotted lines denote those data for the different molecular weight samples in dilute solutions, which are estimated by using the critical concentrations evaluated from eq 2b and assuming that $J_e \propto M/C$, except for the value of the F-128 sample directly obtained from experiments in previous work.⁸ It is apparent from this figure that the $J_e C$ data measured here are almost constant for each sample and agree with the corresponding dotted lines, though they somewhat scatter. Moreover, if we calculate the reduced steady-state compliance J_{eR} defined as $(J_e CRT/M)\{\eta^{02}/(\eta^0 - \eta_s)^2\}$, where R is the gas constant and T is the absolute temperature, the J_{eR} data in this work are almost independent of molecular weight and concentration and agree well with the data in dilute solutions for J_e .^{1,2,6,8,9} Thus, it is confirmed that the concentration and molecular weight dependences of J_e in this work can be expressed as $J_e \propto M/C$, and hence the concentration region in this experiment is the semidilute solution for η^0 but the dilute solution for J_e .

The transient viscosity $\eta^r(t|\dot{\gamma})$ may be defined by

$$\eta^r(t|\dot{\gamma}) \equiv P_{21}^r(t|\dot{\gamma})/\dot{\gamma} = \int_{-\infty}^{\infty} \tau H(\tau) \exp(-t/\tau) d \ln \tau \quad (4)$$

where $P_{21}^r(t|\dot{\gamma})$ is the shear stress at time t after cessation of steady shear flow, of which the rate of shear is $\dot{\gamma}$, $H(\tau)$ is the relaxation spectrum, and τ is the relaxation time. If $\dot{\gamma}$ is low enough, $\eta^r(t|\dot{\gamma})$ composes a single line irrespective of $\dot{\gamma}$ as reported previously.^{14,15} By assuming a discrete distribution of relaxation times,^{5,16} $\eta^r(t|\dot{\gamma})$ at the longest time end can be written as

$$\eta^r(t|\dot{\gamma}) = \tau_m G_m \exp(-t/\tau_m) \quad (5)$$

where τ_m is the longest relaxation time and G_m is the corresponding relaxation strength. Figure 2 shows an example of the time dependence of $\eta^r(t|\dot{\gamma})$ plotted in the form of $\log \eta^r(t|\dot{\gamma})$ against t . From the slope of asymptotic line at the longest time end and the intercept of the line at $t = 0$ in the figure, therefore, we can evaluate τ_m and the product of τ_m and G_m . The τ_m and $\tau_m G_m$ data thus obtained are listed in Table II.

Both τ_m and G_m can be also evaluated from the asymptotic line of $\log G(t)$ vs T , where $G(t)$ is obtained by using the relationship, $G(t) = -d\eta^r(t|\dot{\gamma})/dt$.⁵ The values thus evaluated are in good agreement with those from η^r . This fact indicates the consistency of the experimental data in the range of long times.

Discussion

In Figure 3 τ_m data are plotted against the corresponding τ_w data. Since the J_e value for F-380 at $C = 3.75$ g/

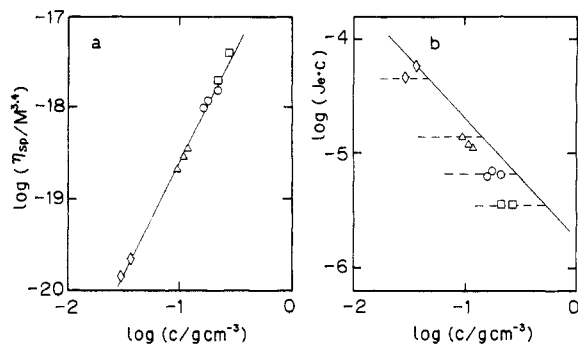


Figure 1. Concentration dependences of zero-shear viscosity η^0 (a) and steady-state compliance J_e (b) for polystyrenes in BBP at 50 °C. The symbols \square , \circ , Δ , and \diamond denote the data of F-40, F-80, F-128, and F-380, respectively.

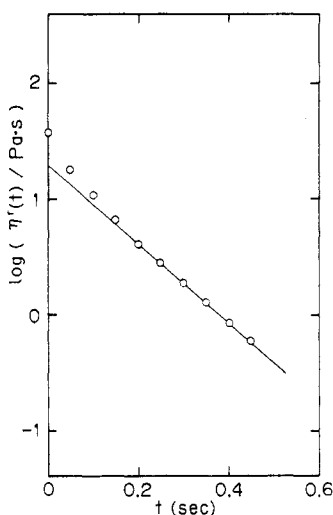


Figure 2. An example of the time dependence of transient viscosity of polystyrene in BBP at 50 °C. The sample is F-128, and the concentration is 9.83 g/dL.

dL is much higher than the J_e value calculated from an average value of J_{eR} (0.28₇) owing to experimental errors in determining J_e as seen in Table I, the τ_w value evaluated by using the J_e value calculated from the average J_{eR} value is employed in place of the experimental τ_w in this case. In this figure we can observe a good proportionality between τ_m and τ_w . The proportionality factor is about 2. To confirm that the both relaxation times have the same functional form, moreover, all the τ_m data are plotted against C in the form of $\tau_m/M^{4.4}$ according to the molecular weight and concentration dependence of τ_w in Figure 4. The straight lines are drawn with a slope of 4. Apparently, the molecular weight and concentration dependences of τ_m and τ_w are the same. Thus, we can conclude that τ_w is well represented by τ_m even in this region.

Finally, we will discuss the relative contribution of the longest relaxation process to the zero-shear viscosity, $\tau_m G_m/\eta^0$, in this region, in comparison with those in the highly entangled regions and theoretical values. Figure 5 shows double-logarithmic plots of $\tau_m G_m/\eta^0$ vs CM in the entangled regions for η^0 over a wide range of entanglement density. Data of poly(α -methylstyrenes) in melts⁴ and data of polystyrene-diethyl phthalate solutions in a highly entangled region ($CM \gg 1.4 \times 10^5$)⁵ are also shown in this figure. It is clear from this figure that most of the data are around 0.6, and there is no distinct difference between the data before and after the critical CM value for J_e . Thus, the magnitude of contribution

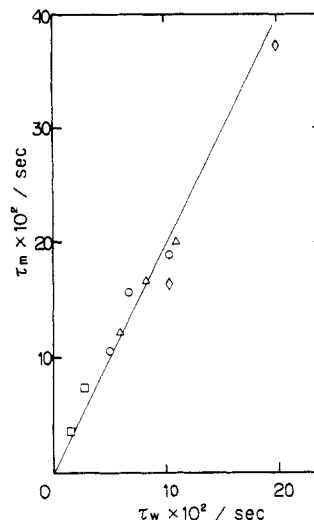


Figure 3. Relationship between τ_m and τ_w . The calculated τ_w value is employed for F-380 at $C = 3.75 \text{ g/dL}$. The symbols are the same as in Figure 1.

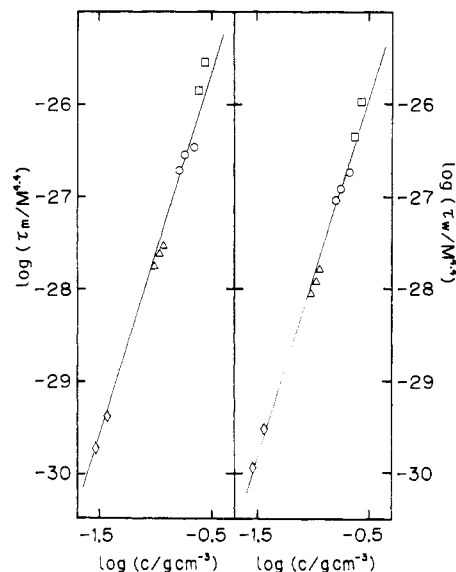


Figure 4. Molecular weight and concentration dependences of τ_m and τ_w . The symbols are the same as in Figure 1.

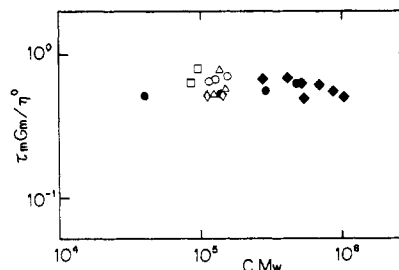


Figure 5. Double logarithmic plots of $\tau_m G_m/\eta^0$ against CM_w . The symbols \bullet and \blacklozenge denote the data of poly(α -methylstyrenes) in melts⁴ and polystyrenes in diethyl phthalate,⁵ respectively. The other symbols are the same as in Figure 1.

of $\tau_m G_m$ to η^0 does not significantly change with the entanglement density.

The theoretical $\tau_m G_m/\eta^0$ values of Zimm,^{1,2} Rouse,^{1-3,16} and Doi-Edwards¹⁷ are 0.42, 0.62, and 0.99, respectively, and the experimental values are close to the theoretical value of Rouse. On the other hand, the theoretical τ_m/τ_w values of Zimm, Rouse, and Doi-Edwards are 2.05,

1.52, and 1.01, respectively, and the experimental values are close to the theoretical value of Zimm. Considering the experimental errors in these viscoelastic parameters, we cannot discuss the difference between Zimm-like and Rouse-like behavior. Moreover, our experimental concentration range may not be appropriate to compare the observed data with these theories. However, it is to be noted that the longest relaxation process in this concentration region is not so much isolated from others as in the case of Doi-Edwards theory.

In summary, we can conclude that the weight-average relaxation time τ_w of linear polymers in semidilute solutions for η° can be well represented by the longest relaxation time τ_m , whether the entanglements are effective to J_e or not.

References and Notes

- (1) Graessley, W. W. *Adv. Polym. Sci.* **1974**, *16*, 1.
- (2) Ferry, J. D. *Viscoelastic Properties of Polymers*, 3rd ed.; Wiley: New York, 1980; Chapters 10, 13, 17.
- (3) Tobolsky, A. V.; Aklonis, J. J.; Akevali, G. *J. Phys. Chem.* **1965**, *42*, 723.
- (4) Fujimoto, T.; Ozaki, N.; Nagasawa, M. *J. Polym. Sci., Polym. Phys. Ed.* **1968**, *6*, 129.
- (5) Osaki, K.; Fukuda, M.; Kurata, M. *J. Polym. Sci., Polym. Phys. Ed.* **1975**, *13*, 775.
- (6) Sakai, M.; Fujimoto, T.; Nagasawa, M. *Macromolecules* **1972**, *5*, 786.
- (7) Takahashi, Y.; Isono, Y.; Noda, I.; Nagasawa, M. *Macromolecules* **1985**, *18*, 1002.
- (8) Takahashi, Y.; Noda, I.; Nagasawa, M. *Macromolecules* **1985**, *18*, 2220.
- (9) Takahashi, Y.; Umeda, M.; Noda, I. *Macromolecules* **1988**, *21*, 2257.
- (10) Isono, Y.; Fujimoto, T.; Takeno, N.; Kajiura, H.; Nagasawa, M. *Macromolecules* **1978**, *11*, 888.
- (11) Endo, H.; Nagasawa, M. *J. Polym. Sci., Polym. Phys. Ed.* **1970**, *8*, 371.
- (12) Sakai, M.; Fukaya, H.; Nagasawa, M. *Trans. Soc. Rheol.* **1972**, *16*, 635.
- (13) Kajiura, H.; Endo, H.; Nagasawa, M. *J. Polym. Sci., Polym. Phys. Ed.* **1973**, *11*, 2371.
- (14) Kajiura, H.; Sakai, M.; Nagasawa, M. *Trans. Soc. Rheol.* **1974**, *18*(2), 323; **1976**, *20*(4), 575.
- (15) Takahashi, Y.; Isono, Y.; Noda, I.; Nagasawa, M. *Macromolecules* **1987**, *20*, 153.
- (16) Tobolsky, A. V.; Murakami, K. *J. Polym. Sci.* **1959**, *40*, 443.
- (17) Doi, M.; Edwards, S. F. *The Theory of Polymer Dynamics*; Oxford University Press: Oxford, 1986; Chapter 7.

Effect of Hydrostatic Pressure on Polystyrene Diffusivity in Toluene

Benny D. Freeman,[†] David S. Soane,^{*‡} and Morton M. Denn

Center for Advanced Materials, Lawrence Berkeley Laboratory, and Department of Chemical Engineering, University of California, Berkeley, Berkeley, California 94720.
Received September 6, 1988; Revised Manuscript Received April 25, 1989

ABSTRACT: The pressure dependence of the mutual diffusion coefficient of selected polystyrene-in-toluene solutions is determined by dynamic light scattering. Decreases in the observed diffusivity with pressure can be explained by changes in the polymer concentration (due to solution compression) and decreases in the solvent fluidity (due to lowering of the system free volume). Quantitative correlations of diffusivity are established for different polymer concentrations and molecular weights, and the results are compared with theoretical predictions.

Introduction

Polymer diffusion at elevated pressures is relevant to many industrial processes, including polymerization reaction engineering and enhanced oil recovery. Furthermore, determination of the mobility of macromolecules at high pressures is important to the understanding of the molecular processes governing polymer rheology and related dynamic processes. Quantitative measurements of polymer diffusion coefficients at different pressures, for example, help to establish the relative importance of system free volume (and thus fluidity) and entanglement effects influence (dictated primarily by polymer concentration and molecular weight). In this work, we determine polymer mutual diffusion coefficients in binary solutions at elevated hydrostatic pressures by dynamic light

scattering, in order to isolate these two possible factors affecting macromolecular mobility.

In a binary solution the mutual diffusion coefficient is defined as the proportionality constant between the component flux and the negative of the component concentration gradient:¹

$$J_i = -D \nabla c_i \quad (1)$$

where J_i is the component flux (in mass of component i per unit area per unit time) in the volume-fixed frame of reference and ∇c_i is the concentration gradient (in mass of component i per unit volume per unit length). Conventionally, component 1 is the solvent and component 2 is the solute. In this paper for simplicity, we delete the subscript and use c to represent the polymer concentration.

Diffusion is in fact driven by free energy gradients from the theory of irreversible thermodynamics and the fact that the chemical potential of polymer solutions can be expressed in terms of the osmotic pressure, π . One obtains

[†] Current address: Department of Chemical Engineering, North Carolina State University, Raleigh, North Carolina 27695.

[‡] To whom correspondence should be addressed at the Department of Chemical Engineering.